E-ISSN: 2664-6773
P-ISSN: 2664-6765
Impact Factor: RJIF 5.6
IJCBS 2024; 6(2): 144-152
www.chemicaljournal.org
Received: 08-10-2024
Accepted: 12-11-2024

Ahmed S Faihan
Department of Chemistry, College of Science, Tikrit University, Tikrit, Iraq

Foud Nihad Abed
Department of Chemistry, College of Science, Tikrit University, Tikrit, Iraq

Reza Behjatmanesh-Ardakani
Department of Chemical Engineering, Faculty of Engineering, Ardakan University, PO Box 184, Ardakan, Iran

Corresponding Author:
Ahmed S Faihan
Department of Chemistry, College of Science, Tikrit University, Tikrit, Iraq

Synthesis, characterization, and computational study of mixed ligand complexes of N-Phenyl-N-(2-thiazoyl) thiourea Pt (II) and tertiary phosphine ligands

Ahmed S Faihan, Foud Nihad Abed and Reza Behjatmanesh-Ardakani

DOI: https://doi.org/10.33545/26646765.2024.v6.i2b.115

Abstract
This project details the synthesis and characterization of three complexes. The precursor ligand was synthesized by reacting 2-aminothiazole with phenyl isothiocyanate to get N-Phenyl-N-(2-thiazoyl) thiourea ($PTTH^2$). Upon reacting the ligand with the [Pt(diphos)Cl_2] complex, the two thioamide protons were deprotonated, yielding complexes of the generic type [Pt(diphos) (PTT)]. Furthermore, the newly synthesized compounds were characterized using various spectroscopic techniques, including FT-IR and 1H-NMR. Both procedures validated the deprotonation of the two N-H protons. The FT-IR spectra indicated the existence of characteristic phosphine bands. Additionally, the ligand $PTTH^2$ and the complex [Pt(PPh_3)$_2$ (PTT)] were subjected to theoretical analysis, and their quantum parameters were assessed. The quantum calculations indicated that the Pt complexes possess a square planar shape with distorted angles.. Also, the 4d orbital of Pt(II) is highly diffused due to the interaction between the P, S, and N donor atoms with Pt ion. The HOMO and LUMO of $PTTH^2$ are spread among all atoms, having a HOMO-LUMO gap of 4.63 eV. The HOMO of [Pt(PPh_3)$_2$ (PTT)] is predominantly localized on nitrogen, sulfur, and certain benzene rings, whereas the LUMO is primarily associated with platinum and other benzene rings. The HOMO-LUMO gap is equal to 3.22 eV, which is near to some semiconductors such as TiO_2 anatase phase. Finally, the prepared complexes were tested against five bacterial species, and showed significant antibacterial action on most of them.

Keywords: Characterization, ligand, phosphine, platinum, quantum

Introduction
Thioureas and their derivatives have garnered significant attention in chemistry owing to their many chemical applications and distinctive physicochemical properties [1, 2]. Thiourea moieties are valuable molecules employed as building blocks in the synthesis of many heterocyclic compounds with multiple uses in chemistry and biology [3, 4]. The versatility and straightforward synthesis of thiourea have facilitated the creation of various innovative anticancer medicines with unique mechanisms of action. Moreover, thioureas exhibit remarkable biological activity as insecticides, fungicides, antivirals, and plant growth regulators, rendering them highly valuable in medicinal chemistry [5]. The isolation of metal ions is a singular use of their function as selective analytical reagents [6]. Thiourea is significant in anion sensing and identification due to the hydrogen-bond donor potential [7, 8]. Thioureas are favored in chemistry due to their readily available precursors, often yielding high-purity products. Furthermore, the chemical, physical, and biological activities of thioureas are enhanced by the easily accessible alkyl groups added to the mother molecules [9] (Figure 1).
Aside from their applications, thioureas have long been utilized as ligands, they are compelling because to their extensive structural diversity, which arises from conformational isomerism, and the availability of several donor sites, including the thiocarbonyl group and the nitrogen atoms.
Derivatives of acylthiourea, can establish monodentate or bidentate chelating interactions with diverse metal ions in various coordination states [10]. Thiourea ligands are generally acknowledged for their role as reducing agents for numerous metal ions. They can bind in various protonation states, including neutral ligands, monoanions, or dianions, and they reduce Cu(II) to Cu(I), Au(III) to Au(I), and Te(IV) to Te(II) [11, 12]. Complexes of zinc(II), cadmium(II), lead(II), copper(I), cobalt(II), and nickel(II) exemplify metals that can coordinate with these neutral, monodentate ligands, resulting from the interaction of the sulfur atom and its lone pairs to create a six-membered ring [13].

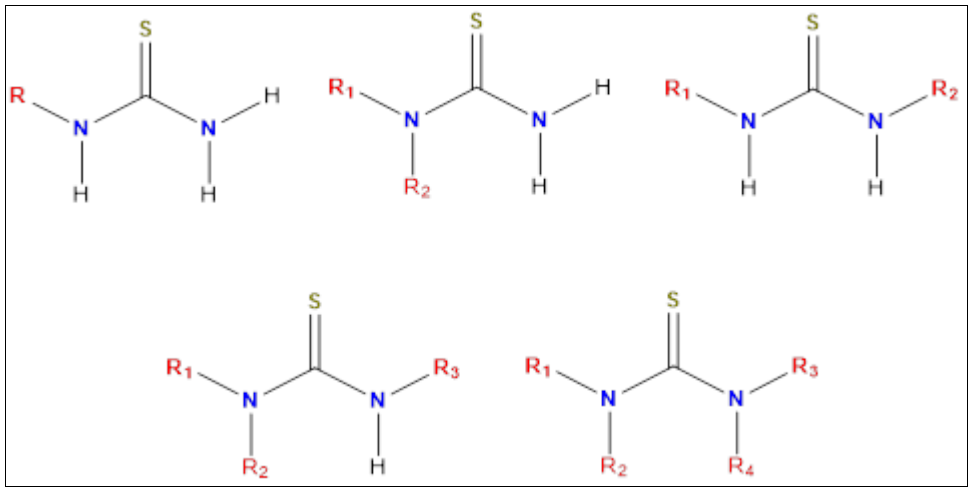

Fig 1: Types of thioureas

Since the thiourea ligand N-Phenyl-N-(2-thiazoyl) thiourea ($PTTH^2$) has shown interesting structural characteristics in a previous publication [14], in which it gave cis and trans conformations with Pt(II) and Pd(II) ions, It is interesting to synthesis mixed ligand complexes derived from $PTTH^2$ with tertiary phosphine ligands. Also, our second target is to study the $PTTH^2$ metal complexes theoretically to determine its catalytic possibilities.

Materials and Instrumentation

Melting points were determined using a Gallenkamp melting point equipment and were uncorrected. The infrared spectra (in KBr pellets) were obtained using a Shimadzu FT-IR 8400 spectrophotometer within the 400-4,000 cm-1 range. NMR spectra were obtained (DMSO-d^6) on a Bruker (400MHz) NMR spectrometer utilizing TMS as an internal standard: triphenylphosphine (PPh3), Bis(diphenylphosphino)methane (dppm), 1,1'-ferrocenyl-bis(diphenylphosphine) (dppf), 2-aminothiazole, phenyl isothiocyanate, and potassium tetra chloroplatinate were acquired from commercial suppliers and employed without further modification. N-Phenyl-N-(2-thiazoyl)thiourea ($PTTH^2$) was synthesized using a modified literature approach [14].

Experimental section

Synthesis of the complexes [Pt(PTT)(diphos)](1-3)

General procedure for the synthesis of 1-3

A stirred solution of dichloro[diphos] platinum (II) complex (0.1 mmol) in 10 ml of dichloromethane was treated with a basic solution of PTTH2 (10 mmol) in ethanol. Upon completion of the addition, the color promptly transitioned to yellow. The reaction was refluxed for one hour. The solution was thereafter put into a 25 ml beaker and permitted to evaporate gradually at ambient temperature. Following a two-day period, the target products were acquired as a yellow to orange solid.

[Pt(dppm)(PTT)] (1) yellow solid (0.0625 g, 77% yield)

[Pt(dppf)(PTT)] (2) Orange solid (0.0842 g, 86% yield)

$[Pt(PPh_3)_2(PTT)]$ (3) Orange solid (0.0624 g, 65% yield)

Results and Discussion

Complexes (1-3) were produced according to the basic technique (Scheme 1), the reaction mixture was refluxed for one hour, resulting in a pale yellow solution. A yellow to orange solid of the desired complexes was produced through the gradual evaporation of the mother solution.

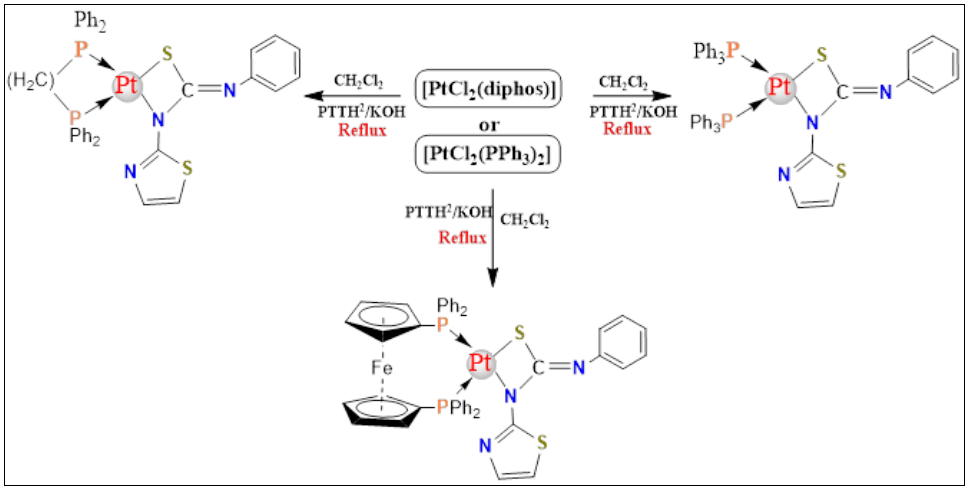

Scheme 1: General route for the synthesis of (1-3) complexes.

The synthesized complexes were characterized by elemental analysis (Table 1) and different spectroscopic techniques including: FT-IR spectroscopy (Table2), and ^{1}H-NMR

Table 1: Physical properties, elemental analysis and yield% for the synthesized complexes (1-3)

#	Complexes	Color	Yield (%)	Elemental analysis (%) Found (Calc.)		
				C	H	N
1.	[Pt(PTT)(dppm)]	yellow	65	53.64 (53.37)	3.55 (3.77)	4.72 (4.91)
2.	[Pt(PTT)(dppf)]	orange	62	53.74 (53.89)	4.03 (3.94)	4.97 (4.83)
3.	[Pt(PTT)(PPh_3)$_2$]	yellow	75	54.53 (54.39)	4.23 (4.11)	4.34 (4.56)

Table 2: Selected infrared stretching vibration bands (Cm^{-1}) of the synthesized complexes (1-3) and $PTTH^2$

#	Compounds	υ(N-H)	υ(C-H) Aromatic	υ(C-H) aliphatic	Phosphine bands			Thioamide bands			
					υ(P-C)	υ(P-C)	υ(P-Ph)	I	II	III	IV
1.	$PTTH^2$	3157, 3414	3080	-----	----	----	---	1626	1554	1184	1130
2.	[Pt(PTT)(dppm)]	----	3051	2854-2953	509	1103	1450	1570	--	---	724
3.	[Pt(PTT)(dppf)]	----	3055	------	493	1097	1438	1575	--	---	748
4.	[Pt(PTT)(PPh_3)$_2$]	----	3051	-------	518	1095	1437	1487	--	---	750

Using IR spectroscopy, the synthesized complexes (1-3) exhibited no thioamide proton absorption bands of the parent ligand N-Phenyl-N-(2-thiazoyl) thiourea ($PTTH^2$), which are observed at 3157 and 3414 cm^{-1}. Furthermore, the coordinated P atoms to Pt(II) was established by the emergence of three different phosphine peaks, which are seen at 493-518 cm^{-1} and 1095-1103 cm^{-1} are ascribed to the υ(P-C) in phosphines [15]. The third phosphine band emerged in the 1437-1450 cm^{-1} range, attributable to the υ(P-Ph) absorption band [16]. Figures 2, 3, and 4 illustrate the IR spectra of the Pt(II) thiourea dianion.

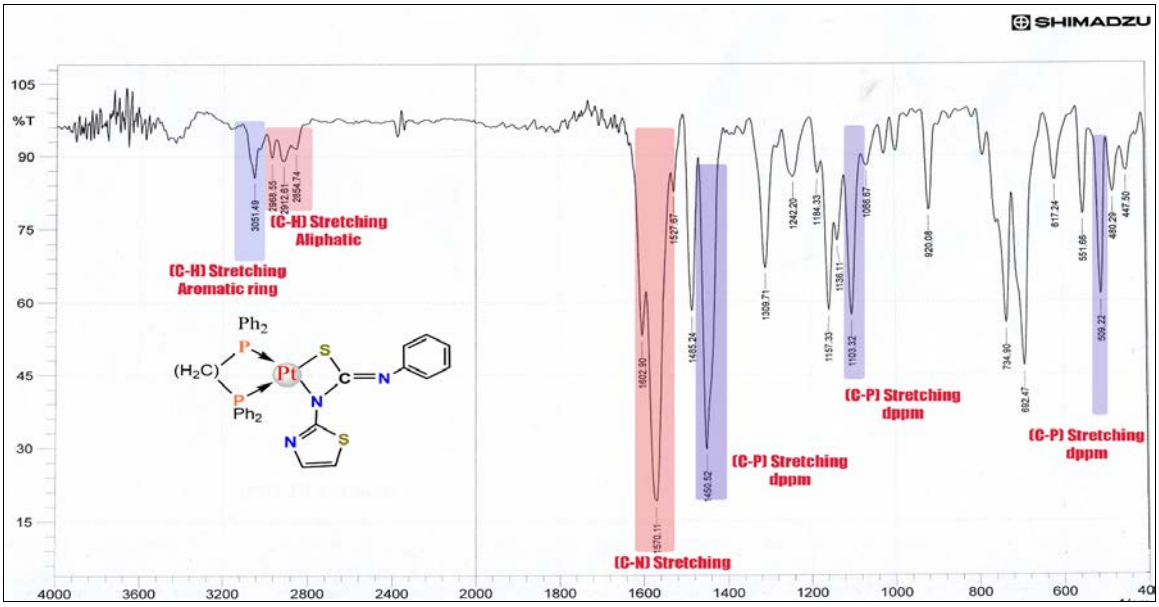

Fig 2: The FT-IR chart of [Pt(PTT) (dppm)] (1).

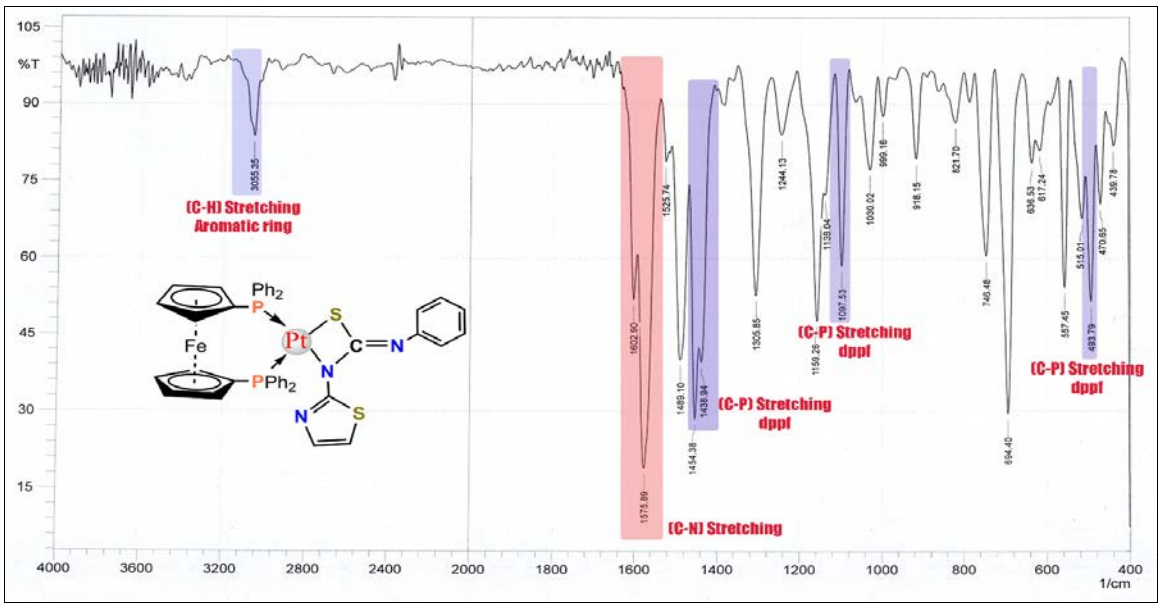

Fig 3: The FT-IR chart of [Pt(PTT) (dppf)] (2).

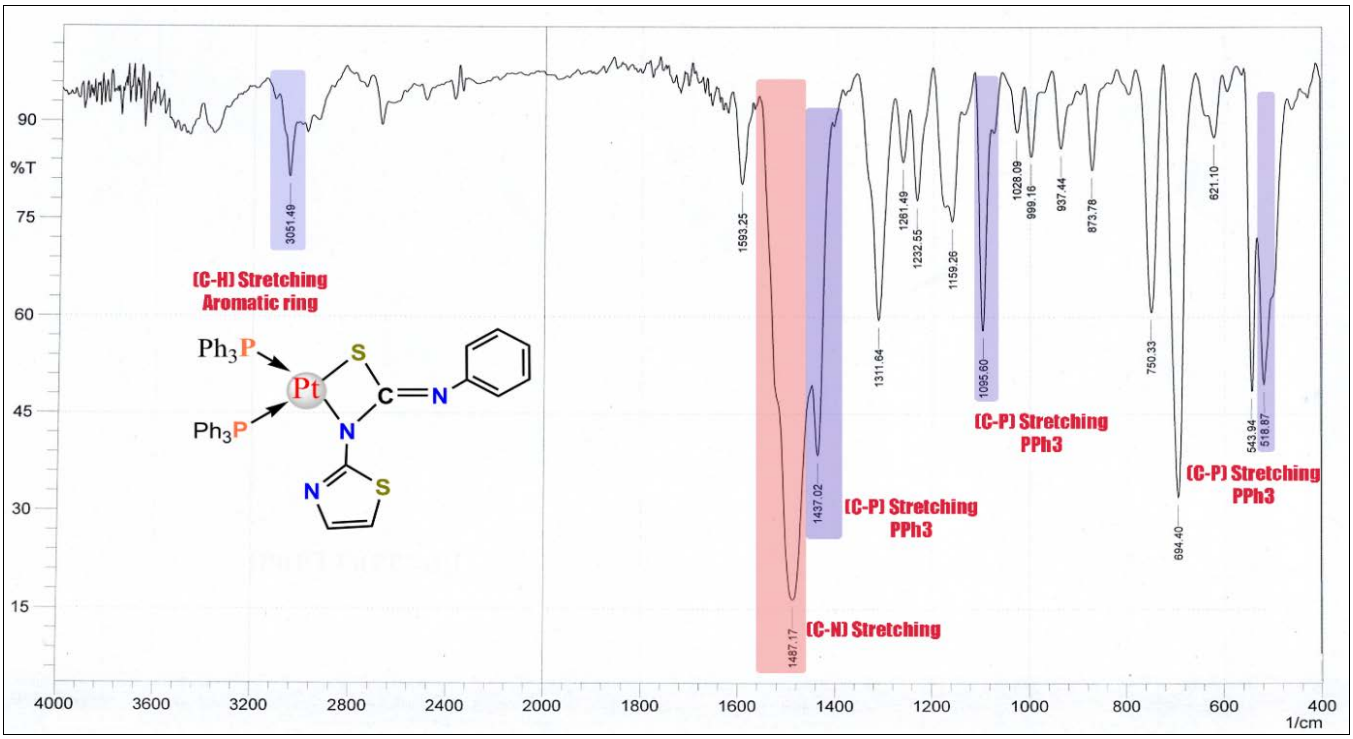

Fig 4: The FT-IR chart of [Pt(PTT) (PPh_3)$_2$] (3).

The ^{1}H-NMR spectrum of complex (1) (Figure 5) showed set of signals within 6-8 ppm range (m, 27 H, Ph + Thiazole). The protons of the alkyl group on phosphine ligand showed as expected which displayed as a singlet at 5.05 ppm (s, 2H, CH_2) which indicates a high-tension ring [17]. Therefore, the best structural pattern should be square planar with platinum being centered.

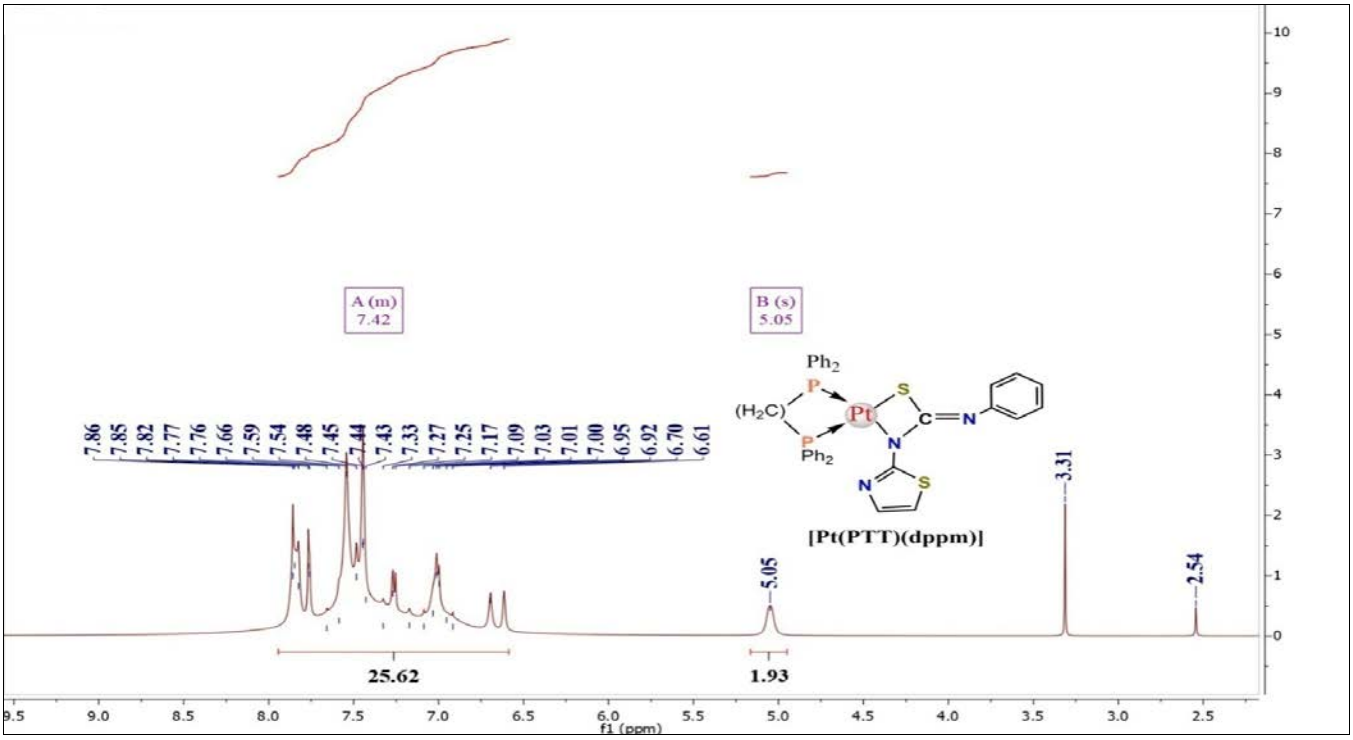

Fig 5: The ^{1}H-nmr chart of [Pt(PTT) (dppm)] (1).

The ^{1}H-NMR spectrum of complex (2) (Figure 6) showed set of signals within 6-8 ppm range that counts for 26 protons. Besides, the protons of the two Cp's ring on the phosphine ligand displayed as three singlets at 4.90, 4.64, and 4.26 ppm (s, 8H, 2Cp).

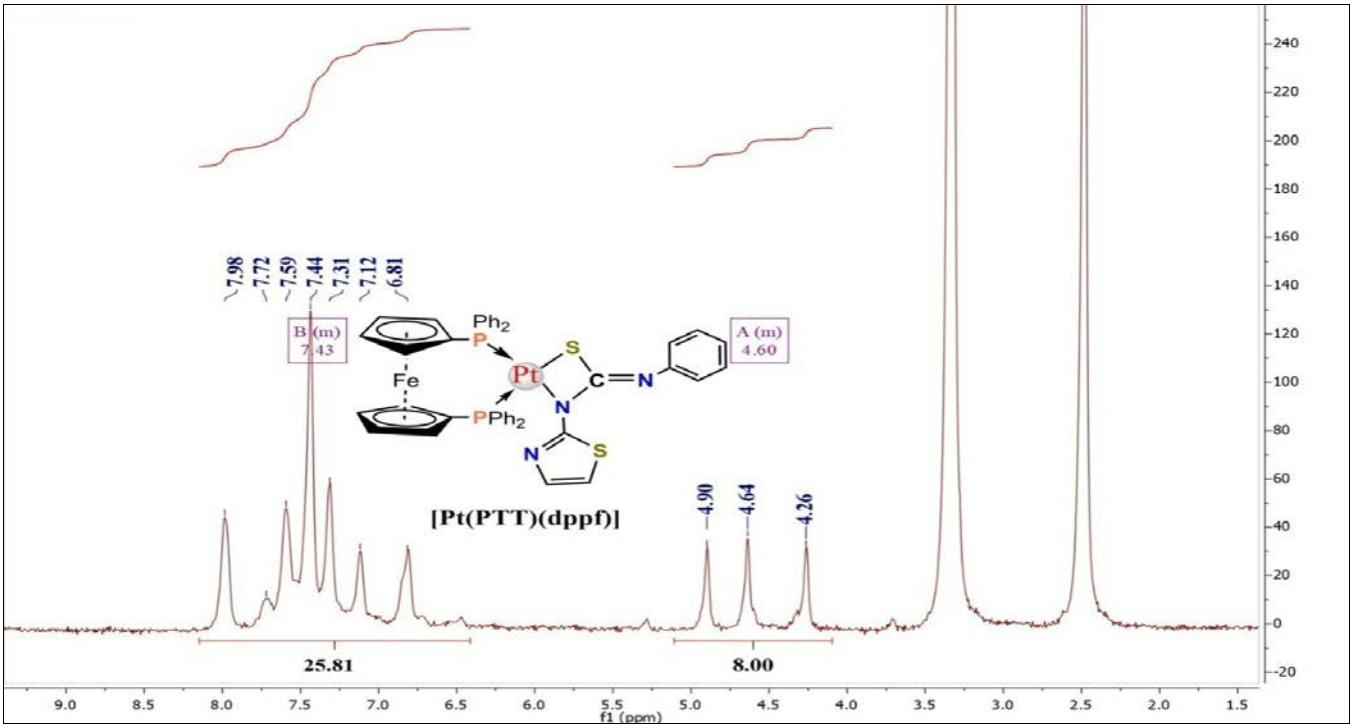

Fig 6: The ^{1}H-nmr chart of [Pt(PTT)(dppf)](2).

The ^{1}H-NMR spectrum of complex(**3**) (Fig. 7) showed set of signals within 6-8 ppm range that belong to the PTT ligand and diphos ligand. Besides, the two protons of the thiazole ring show at 6.43 ppm (d, 2H).

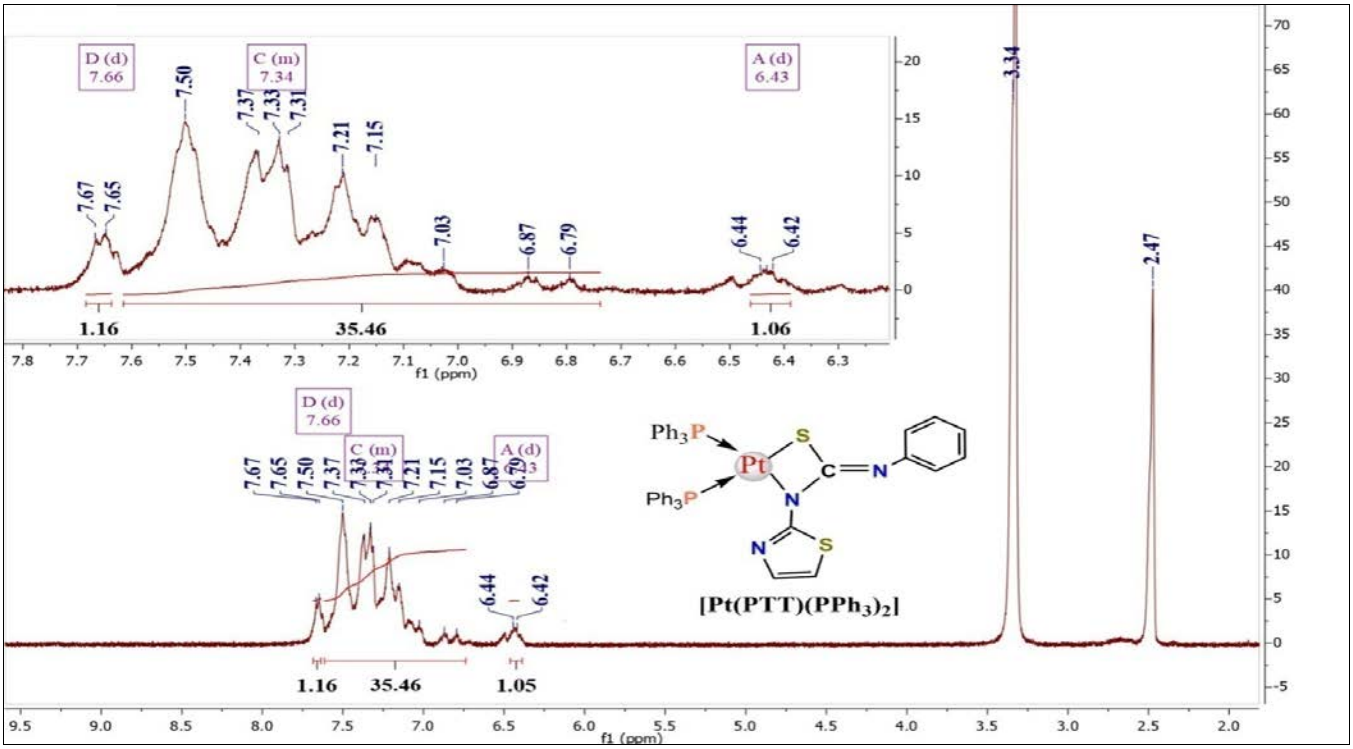

Fig 7: The ^{1}H-nmr chart of [Pt(PTT) (PPh_3)$_2$] (3).

Computational Detail

Electronic structure calculations were done by Gaussian 09 program [18]. B3LYP/Def2-TZVP (triple zeta + polarization) basis set was utilized to obtain more detailed information about the studied compounds. At the first step, the geometrical structures of the ligand (PTTH^2) and the complex (3) were optimized by minimizing the first derivatives of the energy to the coordinates (forces). Then, the second derivatives of the energy to the coordinates (frequencies) were calculated to be sure that the geometries are all in the localminimainthe potential energy surface (PES). All calculated frequencies were positive, so, the geometries are in the local minima. To characterize electron donor and acceptor orbitals, natural bond orbital (NBO) calculations were done by NBO 6.0 program [19]. Gauss View program [20], was used to show the contour plots.

Computational studies

Geometrical and Electronic Properties

Gas phase optimized structures of PTTH^2 and [Pt(PTT)

$(PPh_3)_2$] have been shown in Fig. 8 The ligand is planar, and optimized geometry shows that there is a good resonance between lone pair of electrons on N and S atoms with C=C and C=N double bonds. This resonance between all non-hydrogenic atoms causes the geometry to be planar. The stabilization energies due to these charge transfers have been discussed in the section NBO. The Pt-complex in its local minimum potential energy surface is square planar. However, the angles are not ideal ones. The angles for S-Pt-P1, S-Pt-N, P-Pt-P, and N-Pt-P35 are 90.8˚, 69.2˚, 99.9˚, and 100.6˚, respectively. Pt^{2+} ion is d^8 in its electronic configuration, and for d^8 configuration there are two forms of square planar and tetrahedral for the geometry. In square planar geometry, all d-electrons are paired. The Pt 4d orbitals are highly diffused, so, their interactions with the electron donor orbitals of P, S, and N are high. To be sure that the most stable spin multiplicity is one (i.e. the molecule is non-magnetic case), a separate SCF calculation on the optimized geometry of the complex has been conducted by FHI-aims code [21] with the option of '*spin collinear*'. This option tries to change the total magnetization to find the most stable SCF energy. We started with high magnetization by setting the initial moment to unity for all atoms. Final converged SCF calculation shows that the complex is non-magnetic ($\mu_B = 0$), which is clearly low-spin.

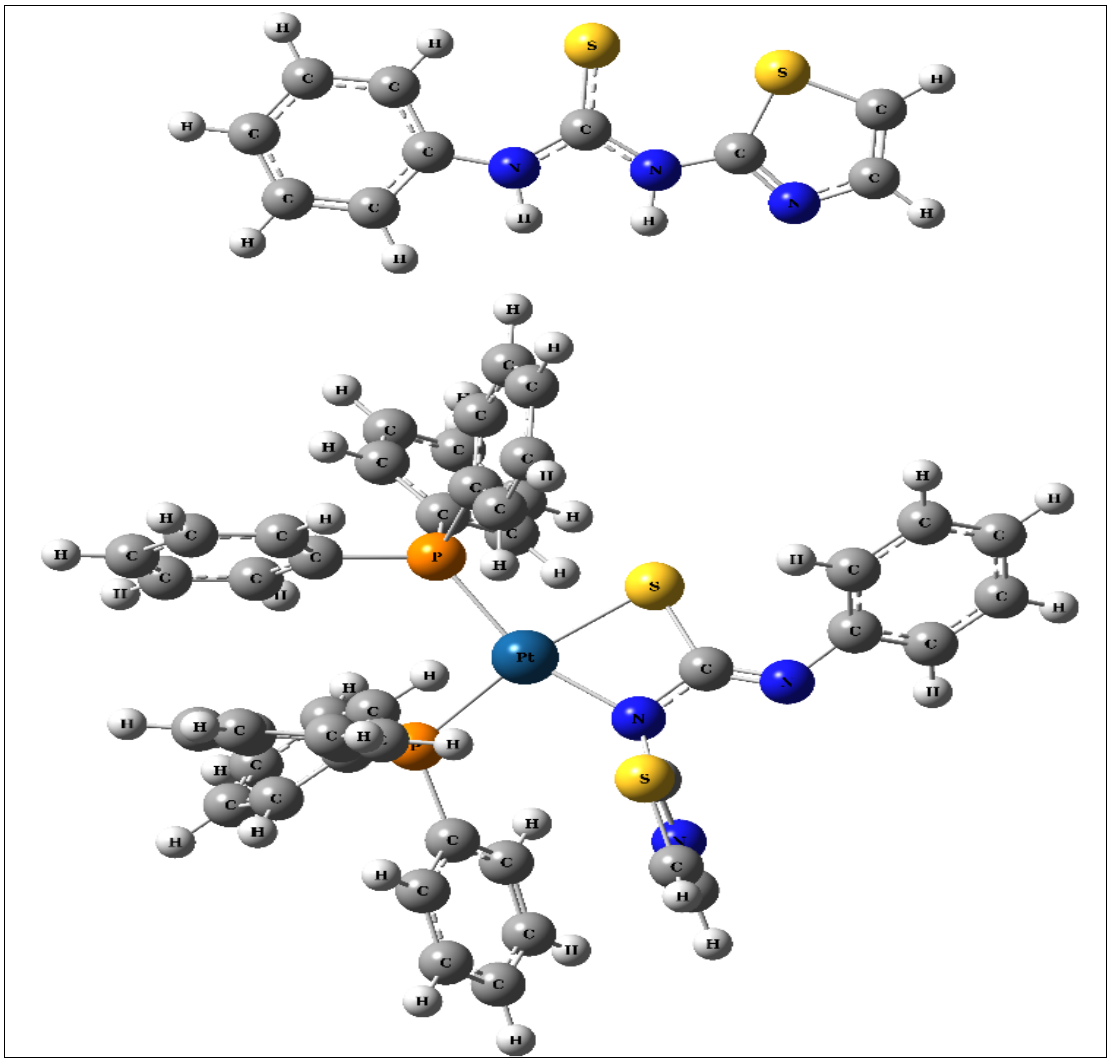

Fig 8: Optimized structure of the ligand ($PTTH^2$) (up) and the complex (3) (down) at the level of B3LYP/Def2-TZVP.

Figure 9 shows the graphical representation of the highest occupied molecular orbital (HOMO) and the lowest unoccupied molecular orbital (LUMO) for the $PTTH^2$and the complex3. For $PTTH^2$, both HOMO and LUMO are distributed on all atoms. Its HOMO-LUMO gap is equal to 4.63 eV which is higher than the semiconductors' band gap. On the other hand, for complex3, The HOMO is mostly localized on nitrogen, sulfur, and select benzene rings, while the LUMO is concentrated on platinum and additional benzene rings. The HOMO-LUMO gap of the compound is 3.22 eV, comparable to some semiconductors like TiO2 in its anatase phase. The (QTAIM) utilizing Bader code [22] indicates that platinum (Pt) possesses a charge of +0.08 eV, whereas phosphorus (P1), phosphorus (P35), nitrogen (N), and sulfur (S) exhibit charges of +1.63 eV, +1.53 eV, -1.03 eV, and -0.23 eV, respectively. It indicates that Pt acquired a charge of 1.92 from both P atoms. N and S atoms function as charge acceptors owing to their electronegativities. The ESP indicates that the sulfur-containing ligand in the complex exhibits a negative ESP, making it a proficient nucleophile, whereas the phosphorus-containing ligand displays a positive PES, rendering it an effective electrophile.

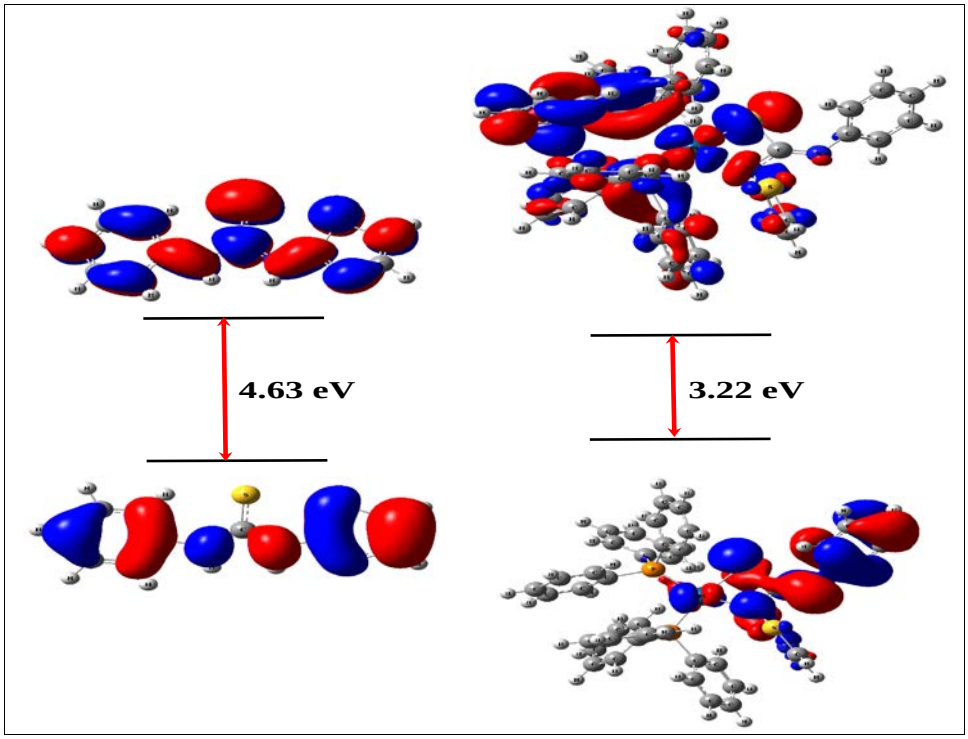

Fig 9: HOMO and LUMO for PTTH[2] and complex3.

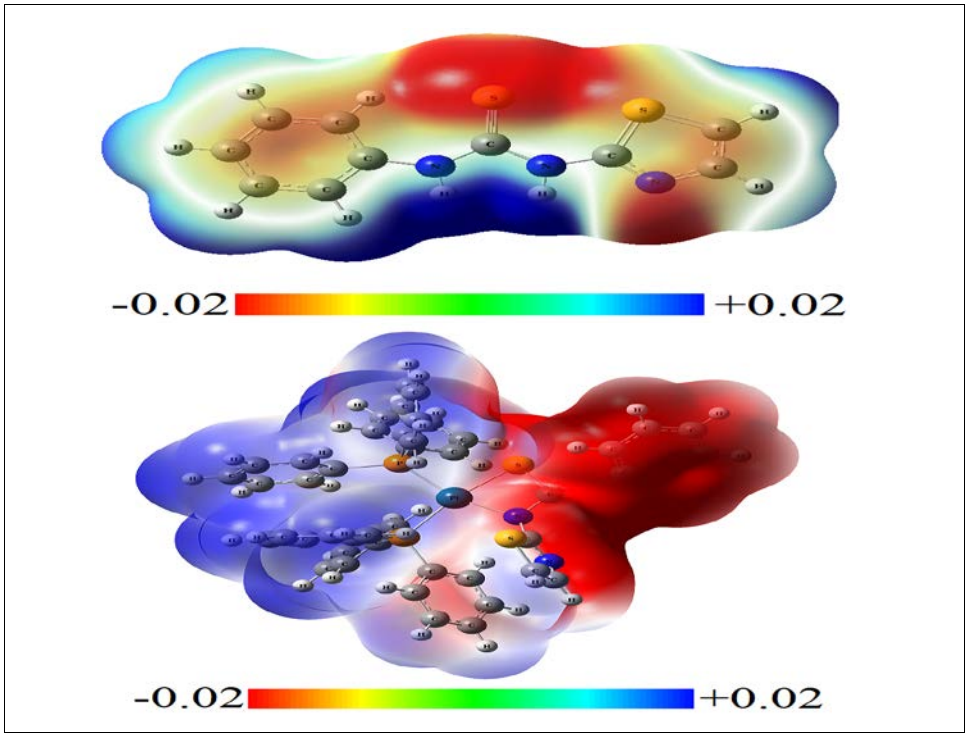

Fig 10: Electrostatic potential (ESP) computed using the B3LYP/Def2-TZVP method for PTTH2 (up) and complex 3 (down) at an iso-surface density value of 0.02 e/Å^3.

NBO Analysis

The natural bond orbital (NBO) calculations were done to obtain more information about electronic resonance and charge transfer stabilization in both PTTH[2]and complex3. In the ligand there are good donor-acceptor charge transfers from both lone pairs (LP) of N and S, and also from π orbitals to the π* orbitals with high second-order perturbation energies (see Table 3). NBO predicts that there is a high electronic resonance in the whole of the molecule. NBO data for the complex 3shows that the LP of donor atoms such as N, S, and P atoms both introduce in the pi-pi electronic resonance and in the gifting their electron to the Pt-contained bonds (see Table 4). There are many high-energy orbitals (Rydberg orbitals) as acceptor orbitals in the NBO output which are not considered in the tables except those for which back-donation are defined. In the back-donation, charge transfers from Pt (or Pt-contained bonds) to the ligands atoms. These charge transfers cause that the charge of Pt to be positive instead of neutral after gaining charges from donor atoms. Figure 11 and 12 represent graphically two highest donor-acceptor orbitals for the PTTH[2] and complex3, respectively.

Table 3: Stabilization energies (second order perturbation energies) from electronic resonance in the PTTH[2] structure.[1]

Donor	type	Acceptor	type	$E^{(2)}$
$(LP2)_{S4}$	100%(p)	$(\pi^*)_{C1-C2}$	55%$(p)_{C1}$+45%$(p)_{C2}$	20.8
$(LP2)_{S4}$	100%(p)	$(\pi^*)_{N3-C5}$	42%$(p)_{N3}$+58%$(p)_{C5}$	33.7
$(LP1)_{N6}$	100%(p)	$(\pi^*)_{N3-C5}$	42%$(p)_{N3}$+58%$(p)_{C5}$	43.2
$(LP1)_{N6}$	100%(p)	$(\sigma^*)_{C9-S22}$	70%$(p)_{C9}$+30%$(p)_{S22}$	71.2
$(LP1)_{N10}$	100%(p)	$(\sigma^*)_{C9-S22}$	70%$(p)_{C9}$-30%$(p)_{S22}$	75.5
$(LP1)_{N10}$	100%(p)	$(\pi^*)_{C11-C13}$	50%$(p)_{C11}$+50%$(p)_{C13}$	33.8
$(\pi)_{N3-C5}$	58%$(p)_{N3}$+42%$(p)_{C5}$	$(\pi^*)_{C1-C2}$	55%$(p)_{C1}$+45%$(p)_{C2}$	21.0
$(\pi)_{C11-C13}$	50%$(p)_{C11}$+50%$(p)_{C13}$	$(\pi^*)_{C12-C14}$	48%$(p)_{C12}$+52%$(p)_{C14}$	18.5
$(\pi)_{C11-C13}$	50%$(p)_{C11}$+50%$(p)_{C13}$	$(\pi^*)_{C15-C16}$	51%$(p)_{C15}$+49%$(p)_{C16}$	21.1
$(\pi)_{C12-C14}$	52%$(p)_{C12}$+48%$(p)_{C14}$	$(\pi^*)_{C11-C13}$	50%$(p)_{C11}$+50%$(p)_{C13}$	20.7
$(\pi)_{C15-C16}$	49%$(p)_{C15}$+51%$(p)_{C16}$	$(\pi^*)_{C12-C14}$	48%$(p)_{C12}$+52%$(p)_{C14}$	22.6

[1]LP means lone pair. Only energies greater than 20 kcal.mol^{-1} were considered. Rydberg (very high energy) orbitals were not considered.

Table 4: Stabilization energies (second-order perturbation energies) resulting from charge transfers between donor and acceptor orbitals in complex 3.1,2. Only donor-acceptors with E(2) over 25 kcal·mol^{-1} were selected.

Donor	type	Acceptor	type	$E^{(2)}$
$(LP1)_{N71}$	100%$(sp^{9.7})^3$	$(\pi^*)_{C72-C73}$	64%$(p)_{C72}$+36%$(p)_{N73}$	41.8
$(LP2)_{N71}$	100%$(sp^{3.16})$	$(\sigma^*)_{P1-Pt69}$	29%$(sp^{2.2})_{P1}$+71%$(sd^{0.9})_{Pt69}$	96.1
$(LP1)_{C79}$	100%(p)	$(\pi^*)_{C75-C77}$	49%$(p)_{C75}$+51%$(p)_{C77}$	97.6
$(LP1)_{C79}$	100%(p)	$(\pi^*)_{C76-C78}$	49%$(p)_{C76}$+51%$(p)_{C78}$	95.5
$(LP2)_{S87}$	~100%$(p)^4$	$(\pi^*)_{C85-N86}$	57%$(p)_{C85}$+43%$(p)_{N86}$	26.1
$(\sigma)_{P1-Pt69}$	71%$(sp^{2.2})$+29%$(sd^{0.9})$	$(\sigma^*)_{Pt69-S70}$	62%$(sd^{1.29})_{Pt69}$+38%$(sp^{9.9})_{S70}$	27.7
$(\sigma)_{Pt69-S70}$	38%$(sd^{1.3})$+62%$(sp^{9.9})$	$(\sigma^*)_{P1-Pt69}$	29%$(sp^{2.2})_{P1}$+71%$(sd^{0.9})_{Pt69}$	54.4
$(LP1)_{P35}$	100%$(sp^{0.9})$	$(\sigma^*)_{P1-Pt69}$	29%$(sp^{2.2})_{P1}$+71%$(sd^{0.9})_{Pt69}$	53.1
$(LP1)_{P35}$	100%$(sp^{0.9})$	$(\sigma^*)_{Pt69-S70}$	62%$(sd^{1.29})_{Pt69}$+38%$(sp^{9.9})_{S70}$	210.5
Back-Donation				
$(LP1)_{Pt69}$	~100%$(d)^5$	$(\sigma^*)_{P1-Pt69}$	29%$(sp^{2.2})_{P1}$+71%$(sd^{0.9})_{Pt69}$	31.4
$(LP1)_{Pt69}$	~100%(d)	$(\sigma^*)_{Pt69-S70}$	62%$(sd^{1.29})_{Pt69}$+38%$(sp^{9.9})_{S70}$	35.5
$(LP1)_{Pt69}$	~100%(d)	$(RY1)_{P35}$	100%$(sp^{11.4}d^{9.2})_{P35}$	40.1
$(LP1)_{Pt69}$	~100%(d)	$(RY2)_{P35}$	100%$(sp^{4.5}d^{6.5})_{P35}$	41.8

[1]LP means lone pair, [2]RY means high-energy unoccupied Rydberg orbitals. They were considered only for back-donation charge transfers due to their importance, [3]9.4% *s* + 90.6% *p*, [4]99.9% *p* + 0.1% *d*, [5]3% *s* + 97% *d*.

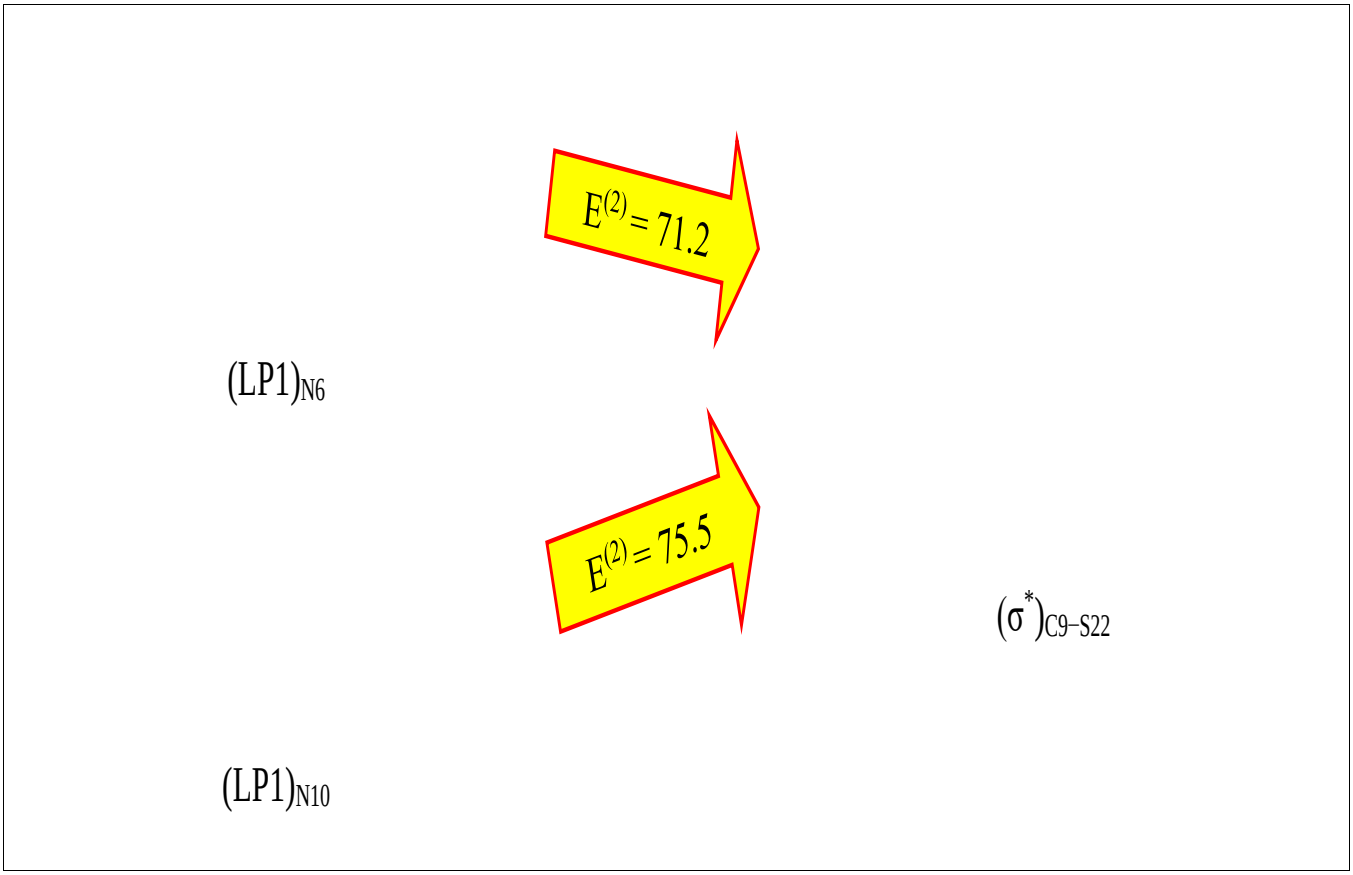

Fig 11: Two highest $E^{(2)}$ donor (left) and acceptor (right) orbitals for PTTH[2]. All units of $E^{(2)}$ are in kcal mol^{-1}. See the Table 1 for more detailed information.

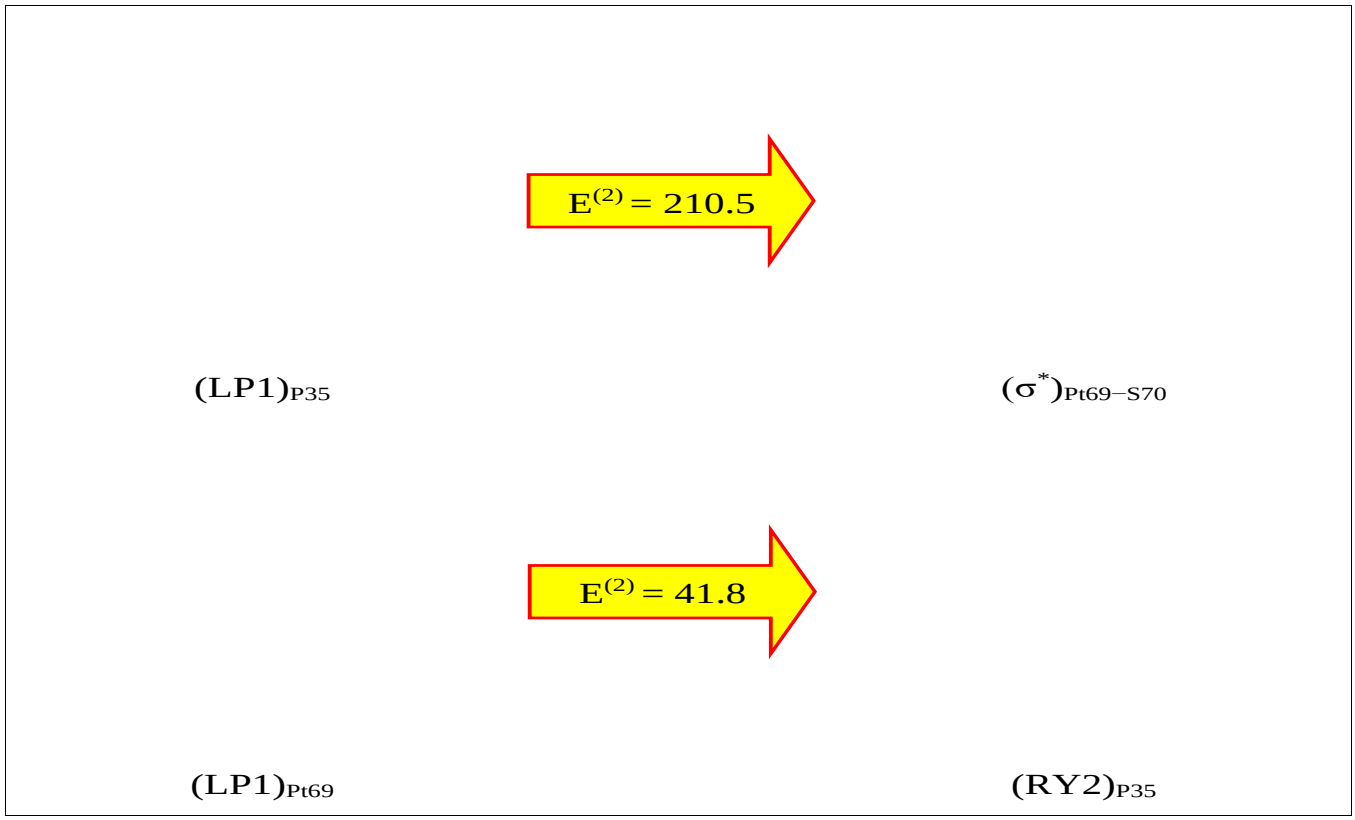

Fig 12: The predominant E(2) donor and acceptor orbitals for complex 3 are depicted; the upper section represents electron donation, while the lower section illustrates electron back-donation. All units of E(2) are expressed in kcal mol^{-1}. Refer to Table 2 for additional specific information.

Conclusions

This study reports the synthesis of three complexes formed from ($PTTH^2$) using various spectroscopic techniques. The reaction of one molar equivalent of [$PtCl_2$(diphos)] (where diphos = dppm or dppf or PPh_3) with one molar equivalent of ($PTTH^2$) in the presence of KOH yielded heterocyclic thiourea dianion complexes of the form [Pt(PTT) (diphos)]. The spectroscopic data analysis indicated that these compounds exhibit square planar shape. Quantum parameters were assessed for both $PTTH^2$ and [Pt(PTT) (PPh_3)$_2$], demonstrating the potential of the Pt(II) complex to function as a catalyst.

References

1. Katritzky AR, Gordeev MF. Journal of the Chemical Society, Perkin Transactions 1. 1991;1:2199-2203.
2. Acharyya R, Dutta S, Basuli F, Peng S-M, Lee G-H, Falvello LR, *et al*. Inorganic Chemistry. 2006;45:1252-1259.
3. El-Ayaan U. Journal of Molecular Structure. 2011;998:11.
4. Affan MA, Salam MA, Ahmad FB, Ismail J, Shamsuddin MB, Ali HM. Inorganica Chimica Acta. 2011;366:227-232.
5. Wang XC, Wang V, Quan ZJ, Wang MG, Li Z. Journal of Chemical Research. 2005;61:689-690.
6. Arslan H, Kulcu N, Florke U. Transition Metal Chemistry. 2003;28:816-819.
7. Duke RM, Gunnlaugsson T. Tetrahedron Letters. 2007;48:8043-8048.
8. Gunnlaugsson T, Kruger PE, Jensen P, Tierney J, Ali HDP, Hussey GM. Journal of Organic Chemistry. 2005;70:10875-10878.
9. Liu WX, Jiang YB. Journal of Organic Chemistry. 2008;73:1124-1127.
10. Yamaguchri A, Penlands B, Mizushimat S, Lane TJ, Rrana C, Quaglian JV. Inorganic Chemistry. 1958;80:527-529.
11. Lenthall JT, Anderson KM, Smith SJ, Steed JW. Crystal Growth & Design. 2007;7:1858-1862.
12. Livingstone SE. Reviews in the Chemical Society. 1965;19:386-425.
13. Saad FA, Buurma NJ, Amoroso AJ, Knight JC, Kariuki BM. Dalton Transactions. 2012;41:4608-4617.
14. Jensen KA, Nrelsen PH. Acta Chemica Scandinavica. 1963;17:1875.
15. Wrrschard GW, Griffin CE. Spectrochimica Acta. 1963;19:1905.
16. Palenik GJ, Mathew M, Steffen WL, Beran G. Journal of the American Chemical Society. 1975;97:1059.
17. Frisch MJ, Trucks GW, Schlegel HB, Scuseria GE, Robb MA, Cheeseman JR, *et al*. Gaussian 09 Revision E.01. Wallingford, CT: Gaussian Inc., 2009.
18. Glendening ED, Landis CR, Weinhold F. NBO 6.0: Natural bond orbital analysis program. Journal of Computational Chemistry. 2013;34:1429-1437.
19. GaussView, Version 5.0. Dennington R, Keith TA, Millam JM. Shawnee Mission, KS: Semichem Inc.; 2016.
20. Blum V, Gehrke R, Hanke F, Havu P, Havu V, Ren X, *et al*. Ab initio molecular simulations with numeric atom-centered orbitals. Computer Physics Communications. 2009;180:2175-2196.
21. Henkelman G, Arnaldsson A, Jónsson H. A fast and robust algorithm for Bader decomposition of charge density. Computational Materials Science. 2006;36:354-360.